RSC Advances

ROYAL SOCIETY OF CHEMISTRY

www.rsc.org/advances

Incorporating Ce^{3+} into a high efficiency phosphor $Ca_2PO_4Cl:Eu^{2+}$ and its luminescent properties

Panlai Li*, Zhijun Wang*, Zhiping Yang, Qinglin Guo

College of Physics Science & Technology, Hebei University, Baoding 071002, China

Abstract: A series of Ce^{3+}, Eu^{2+} and Ce^{3+}/Eu^{2+} doped Ca_2PO_4Cl phosphors are synthesized by a high temperature solid-state method. Not only the emission intensity of $Ca_2PO_4Cl:Eu^{2+}$ is obviously enhanced by codoping Ce^{3+}, but also the spectral profile of excitation band is almost not influenced. The energy transfer from Ce^{3+} to Eu^{2+} in Ca_2PO_4Cl has been validated and proved to be a resonant type via a dipole-dipole interaction. Under the 400 nm radiation excitation, the luminescent intensity of $Ca_2PO_4Cl:Ce^{3+}$, Eu^{2+} is found to be about 200% as high as that of $Ca_2PO_4Cl:Eu^{2+}$, and 300% as high as that of $BaMgAl_{10}O_{17}:Eu^{2+}$. The thermal quenching property reveals that $Ca_2PO_4Cl:Ce^{3+}$, Eu^{2+} has the excellent characteristics. Therefore, $Ca_2PO_4Cl:Ce^{3+}$, Eu^{2+} may have potential application as a blue-emitting phosphor for white LEDs.

Keywords: Luminescence; Phosphors; Energy transfer; White LEDs; $Ca_2PO_4Cl:Ce^{3+}$, Eu^{2+}

1 Introduction

In recent years, there has been growing importance focused on research in light emitting diodes (LEDs) because of their long operation lifetime, energy-saving feature and high material stability [1]. Therefore, white LEDs are promising candidate to replace conventional incandescent and fluorescent lamps. At present, the most wide used method to obtain white emission is the combination of a blue LED chip and a yellow phosphor YAG:Ce. However, the white LEDs exhibit a high correlated color temperature (CCT≈7750 K) and a poor color rendering index (CRI≈70-80), because they are lack of

*li_panlai@126.com
*wangzj1998@126.com

red component [2]. During the past few years, white LEDs fabricated using a near ultraviolet (n-UV) LED (380-420 nm) coupled with red, green and blue phosphors have attracted much attention [3]. The most frequently used blue phosphor for n-UV LED is $BaMgAl_{10}O_{17}:Eu^{2+}$ (BAM) [4]. However, the absorption of BAM for wavelength above 400 nm is quite poor. Accordingly, it is urgent to develop new blue phosphors that could be effectively excited in the n-UV range especially for wavelength of 400 nm [5-7]. For example, Song et al. investigated the luminescent property of $RbBaPO_4:Eu^{2+}$ [8]; Liu et al. synthesized a high efficiency and high color purity blue-emitting phosphor $NaSrBO_3:Ce^{3+}$ [9]. Moreover, in order to effectively improve the luminescence of phosphor, the interest in this field arises because the energy transfer from a donor to an acceptor. Actually, the energy transfer from the donor (sensitizer) Ce^{3+} to the acceptor (activator) Eu^{2+} has been already reported. For example, the energy transfer from Ce^{3+} to Eu^{2+} in $LiSr_4(BO_3)_3$ is studied, and the emission color of phosphor can be tuned by appropriate adjustment of the relative proportion of Ce^{3+}/Eu^{2+}, and the energy transfer mechanism of $Ce^{3+}\rightarrow Eu^{2+}$ in $LiSr_4(BO_3)_3$ is the dipole-dipole interaction [10]. Actually, for many compounds, such as $SrSi_2O_2N_2$, $CaSi_2O_2N_2$, $Ba_{1.3}Ca_{0.7}SiO_4$, $Sr_3Gd(PO_4)_3$, $Ca_9Y(PO_4)_7$, $NaMg_4(PO_4)_3$, $NaMgPO_4$, $Ca_8Gd_2(PO_4)_6O_2$ and $BaMg_2(PO_4)_2$, the similar types of $Ce^{3+}\rightarrow Eu^{2+}$ energy transfer are also observed [11-19]. Obviously, the Eu^{2+} emission can be efficiently enhanced by $Ce^{3+}\rightarrow Eu^{2+}$ energy transfer. Hence, the exploration of material can effectively support our demand and guarantee the continuation of progress. $Ca_2PO_4Cl:Eu^{2+}$ which has the excellent internal and external quantum efficiencies, the intense emission, the high quantum efficiency and excellent thermal stability [20], and may serve as a potential candidate for n-UV LED. Therefore, in the present work, we tentatively introduced Ce^{3+} into $Ca_2PO_4Cl:Eu^{2+}$ to enhance its emission intensity. The energy transfer from Ce^{3+} to Eu^{2+} is systematically studied using the

photoluminescence excitation and emission spectra, and lifetimes, and the thermal quenching property of $Ca_2PO_4Cl:Ce^{3+}$, Eu^{2+} is also investigated.

2 Experimental

2.1 Sample preparation

A series of $Ca_{2-x-y}PO_4Cl:xCe^{3+}$, yEu^{2+} (x, y molar concentration) samples are synthesized by a high temperature solid-state method. The initial materials, including $CaCO_3$ (A.R.), $CaCl_2·6H_2O$ (A.R.), $NH_4H_2PO_4$ (A.R.), CeO_2 (99.99%) and Eu_2O_3 (99.99%), are weighed in stoichiometric proportion, thoroughly mixed and ground by an agate mortar and pestle for more than 30 min till they are uniformly distributed. The obtained mixtures are heated at 1000℃ for 2 h in crucibles along with a reducing atmosphere ($5\%H_2/95\%N_2$), and then are naturally cooled to room temperature. In order to measure the characteristics of the phosphor, the samples are ground into powder.

2.2 Materials characterization

The phase formation is determined by X-ray diffraction (XRD) in a Bruker AXS D8 advanced automatic diffractometer (Bruker Co., German) with Ni-filtered Cu Kα1 radiation (λ=0.15405 nm), and a scan rate of 0.02°/s is applied to record the patterns in the 2θ range from 10° to 70°. The steady time resolved photoluminescence spectra are detected by a FLS920 fluorescence spectrometer, and the exciting source is a 450 W Xe lamp. The curve fittings are performed on the luminescence decay curves to confirm the decay time. The Commission International de I'Eclairage (CIE) chromaticity coordinates of sample are measured by a PMS-80 spectra analysis system. All measurements are carried out at room temperature.

3 Results and discussion

3.1 Phase formation

The XRD patterns of $Ca_2PO_4Cl:Ce^{3+}$, $Ca_2PO_4Cl:Eu^{2+}$ and $Ca_2PO_4Cl:Ce^{3+}$, Eu^{2+} are measured and a similar diffraction patterns are observed for each sample. As a representative, Fig.1 shows the XRD patterns of $Ca_2PO_4Cl:0.03Ce^{3+}$, $Ca_2PO_4Cl:0.07Eu^{2+}$, $Ca_2PO_4Cl:0.03Ce^{3+}$, $0.07Eu^{2+}$. Compared the diffraction data with the standard JCPDS card (No.19-0247), and there has no difference between the doped impurity Ca_2PO_4Cl and the pure Ca_2PO_4Cl. The uniform diffraction patterns indicate that the phase formation of Ca_2PO_4Cl is not influenced by a little amounts of Ce^{3+}, Eu^{2+}, or Ce^{3+}/Eu^{2+}. Ca_2PO_4Cl which crystallizes in the orthorhombic system with space group of pbcm(57) and with four formula units per unit cell (N=4), and the dimensions of unit cell are a=0.6185 nm, b=0.6983 nm and c=1.082 nm [20-25].

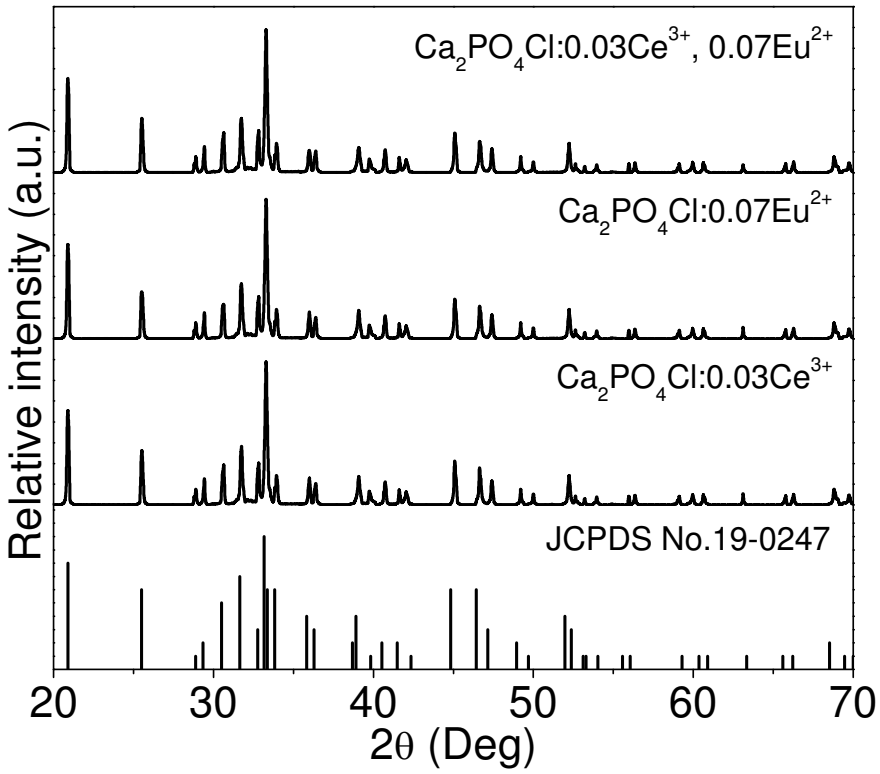

Fig.1. XRD patterns of $Ca_2PO_4Cl:0.03Ce^{3+}$, $Ca_2PO_4Cl:0.07Eu^{2+}$ and $Ca_2PO_4Cl:0.03Ce^{3+}$, $0.07Eu^{2+}$.

The standard data of Ca_2PO_4Cl (JCPDS No. 19-0247) is shown as reference.

3.2 Luminescent properties of Ce^{3+}, Eu^{2+} and Ce^{3+}/Eu^{2+} in Ca_2PO_4Cl

Fig.2a presents $Ca_2PO_4Cl:0.07Eu^{2+}$ has a broad emission band under the 370 nm radiation excitation, and the peak locates at 450 nm which is typically attributed to the $4f^6 5d^1 \rightarrow 4f^7$ electronic dipole allowed transition of Eu^{2+} ion. Because two different crystallographic sites are available for the divalent Ca^{2+} ions, one with site symmetry C_2 and the other with site symmetry C_S. Therefore, Eu^{2+} ions may occupy two different Ca^{2+} sites [20]. The excitation band is observed to mainly consist of unresolved band due to the $4f^7 \rightarrow 4f^6 5d^1$ transition of Eu^{2+} ion. When the Eu^{2+} ions occupy the lattice sites with C_2 or C_S symmetry in Ca_2PO_4Cl, the fivefold degeneracy of the 5d levels is expected in the excitation spectrum. Nevertheless, the dominating bands in the excitation spectrum is difficult to resolve because of serious overlap between 5d levels. The broad excitation band is ascribed to the high covalency of Ca_{Eu}-Cl bonding and large crystal-field splitting. The inset of Fig.2a shows the emission intensity of $Ca_2PO_4Cl:Eu^{2+}$ as function of Eu^{2+} doping content, and the optimal doping content is 0.07 mol.

Fig.2b depicts $Ca_2PO_4Cl:0.03Ce^{3+}$ exhibits a strong broad emission band between 320-500 nm under the 334 nm radiation excitation, and the emission peak locates at 367 nm due to the $4f^0 5d^1 \rightarrow 4f^1$ transition of Ce^{3+} ion. The excitation spectrum shows broad band from 200 to 350 nm, and the peaks locate at 268 nm and 334 nm, respectively, which correspond to the $4f^1 \rightarrow 4f^0 5d^1$ transition of Ce^{3+} ion [20-22]. The inset of Fig.2b presents the emission spectra of $Ca_2PO_4Cl:Ce^{3+}$ with the different Ce^{3+} doping content. The emission spectra have no obvious change in the wavelength and band shape with increasing the Ce^{3+} doping content, which indicated that the crystal-field strength experienced by the activator does not change. In other words, doping into the lattice site does not cause the expansion or shrinkage of the unit cell, as revealed by the XRD data. However,

the emission intensity of $Ca_2PO_4Cl:Ce^{3+}$ is influenced by the Ce^{3+} doping content, and the optimal doping content is 0.03 mol Ce^{3+}, and the concentration quenching effect is also observed.

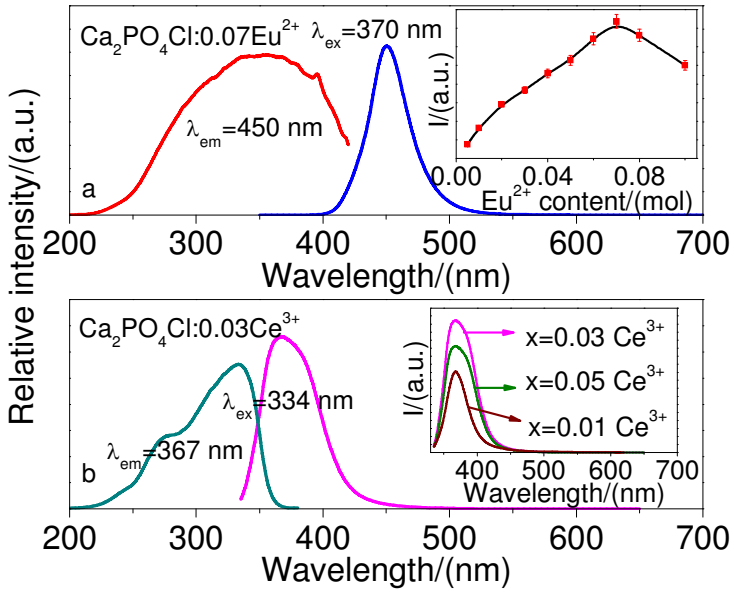

Fig.2. Emission and excitation spectra of (a) $Ca_2PO_4Cl:0.07Eu^{2+}$ and (b) $Ca_2PO_4Cl:0.03Ce^{3+}$.

The inset: (a) the emission intensity of $Ca_2PO_4Cl:0.07Eu^{2+}$ as function of Eu^{2+} doping content (λ_{ex}=370 nm);

(b) the emission spectrum of $Ca_2PO_4Cl:xCe^{3+}$ (λ_{ex}=334 nm).

Generally, the trivalent rare earths ions, such as Ce^{3+}, substitute for the bivalent alkaline earth, such as Ca^{2+}, in the compound, there has the charge unbalance which may result in the formation of defects in the phosphor. Hence the incorporation of alkali metal ions might offset the charge unbalance generated by Ce^{3+} ion substitution for Ca^{2+} ion, reduced the lattice distort, and affected the luminescent properties [26-28]. Among the radii of Li^+, Na^+ and K^+, there has the slightest difference between Na^+ and Ca^{2+} ions, Therefore, Na^+ ion may lead to the slightest negative influence on the luminescence of Ce^{3+} in Ca_2PO_4Cl. Under the 334 nm radiation exciation, the emission spectra of $Ca_2PO_4Cl:0.03Ce^{3+}$, and $Ca_2PO_4Cl:0.03Ce^{3+}$, $0.03Na^+$ are shown in Fig.S1 (Supporting Information). The results present that the two phosphors have the same spectral profile, however, the emission

intensity of Ca_2PO_4Cl:0.03Ce^{3+}, 0.03Na^+ is appreciably stronger than that of Ca_2PO_4Cl:0.03Ce^{3+}. The results indicate that incorporating Na^+ into Ca_2PO_4Cl:Ce^{3+} has no negative influence on the luminescence of Ca_2PO_4Cl Ce^{3+}, to some extent, can enhance its emission intensity. In the present work, the research focuses on the luminescence and energy transfer of Ce^{3+}→Eu^{2+} in Ca_2PO_4Cl. Therefore, the problem of charge compensation is no longer discussed.

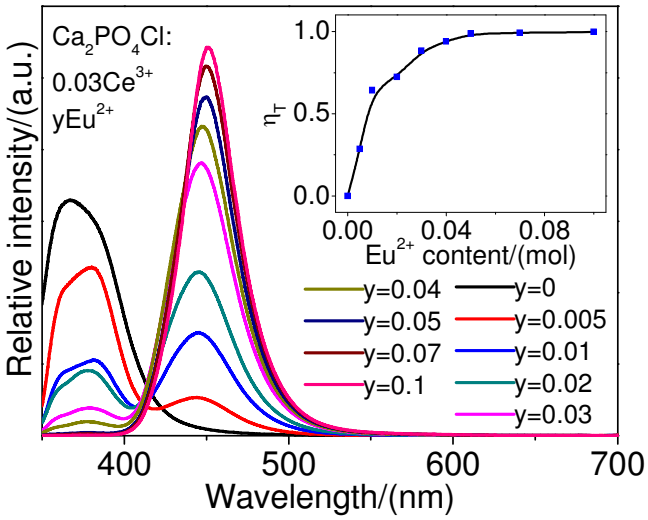

Fig.3. Emission spectra of Ca_2PO_4Cl:0.03Ce^{3+}, $y$$Eu^{2+}$ (λ_{ex}=334 nm).

The inset: variation of η_T for Ca_2PO_4Cl:0.03Ce^{3+}, $y$$Eu^{2+}$ (y=0-0.1) with the Eu^{2+} doping content.

As shown in Fig. 2, there has an obvious spectral-overlap between the emission spectrum of Ce^{3+} and the excitation spectrum of Eu^{2+}, indicating the possibility of energy transfer from Ce^{3+} to Eu^{2+} in Ca_2PO_4Cl. Under the Ce^{3+} 334 nm excitation peak, the spectra of Ca_2PO_4Cl:0.03Ce^{3+}, $y$$Eu^{2+}$ (y=0-0.1) are measured and shown in Fig.3. With the lower Eu^{2+} doping content, there has both Ce^{3+} and Eu^{2+} emission bands, and the emission intensities of Ce^{3+} decrease with increase the Eu^{2+} doping content. With the higher Eu^{2+} doping content, such as 0.05 mol Eu^{2+}, the Ce^{3+} emission disappears, only the Eu^{2+} emission exist in the spectra of Ca_2PO_4Cl:0.03Ce^{3+}, $y$$Eu^{2+}$. The results mean that the energy transfer from Ce^{3+} to Eu^{2+} in Ca_2PO_4Cl is validated. Fig.S2 (Supporting Information) depicts

the emission spectra of Ca_2PO_4Cl:0.07Eu^{2+}, Ca_2PO_4Cl:0.03Ce^{3+}, 0.07Eu^{2+} and $BaMgAl_{10}O_{17}$:Eu^{2+} under the 400 nm radiation excitation. The results obviously present that the luminescent intensity of Ca_2PO_4Cl:Ce^{3+}, Eu^{2+} is found to be about 200% as high as that of Ca_2PO_4Cl:Eu^{2+}, and 300% as high as that of $BaMgAl_{10}O_{17}$:Eu^{2+}.

Generally, the energy transfer efficiency (η_T) from a sensitizer to an activator can be expressed according to Paulose et al. [29]

$$\eta_T=1-(I_S/I_{S0}) \quad (1)$$

where I_{S0} and I_S are the luminescent intensities of the sensitizer in the absence and presence of the activator. In fact, for Ce^{3+}/Mn^{2+}, Eu^{2+}/Mn^{2+}, Ce^{3+}/Eu^{2+} and Ce^{3+}/Tb^{3+} codoped phosphors, the energy transfer efficiency can be easily achieved using Eq.(1) [30-33], generally, the energy transfer efficiency (η_T) from the sensitizer to the activator gradually increases with increase the activator doping content. In the present work, In order to well understand the energy transfer process, using Eq.(1), the energy transfer efficiencies (η_T) $Ce^{3+}\rightarrow Eu^{2+}$ of Ca_2PO_4Cl:Ce^{3+}, $y$$Eu^{2+}$ (y=0-0.1) are calculated, and shown in the inset of Fig.3. As a result, the η_T is found to gradually increase with enhancing the Eu^{2+} doping content. The results mean that the efficient energy transfer $Ce^{3+}\rightarrow Eu^{2+}$ exist in Ca_2PO_4Cl.

For the 450 nm emission of Ca_2PO_4Cl:0.03Ce^{3+}, $y$$Eu^{2+}$, the corresponding excitation spectra are shown in Fig.4. It can be seen from Fig.2, Ca_2PO_4Cl:Eu^{2+} has an obvious absorption in the range of 300-355 nm, and Ca_2PO_4Cl:Ce^{3+} presents a strong excitation band from 300 to 340 nm. However, Ca_2PO_4Cl:Ce^{3+} has weaker absorption in the range of 345-355 nm. Therefore, though the intensity of excitation band (from 330 to 355 nm) increases with enhancing the amount of Eu^{2+} doping content. In fact, the coresponding exciation band which is common to the $4f^7\rightarrow 4f^6 5d^1$ transition of Eu^{2+} ion and the $4f^1\rightarrow 4f^0 5d^1$ transition of Ce^{3+} ion. Hence the increase of intensity (330-355 nm) comes from

the emission of Eu^{2+}, not Ce^{3+}. In other words, the results mean that the excitation characteristics of Ce^{3+} decreases, and that of Eu^{2+} increases. Especially, there has only the excitation characteristics of Eu^{2+} with further increase the Eu^{2+} doping content, *viz.*, the efficient energy transfer from Ce^{3+} to Eu^{2+} ought to exist in Ca_2PO_4Cl.

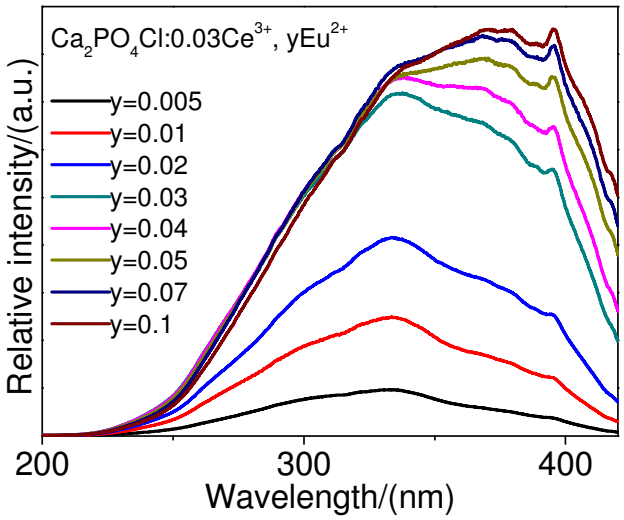

Fig.4. Excitation spectra of $Ca_2PO_4Cl:0.03Ce^{3+}$, yEu^{2+} (λ_{em}=450 nm).

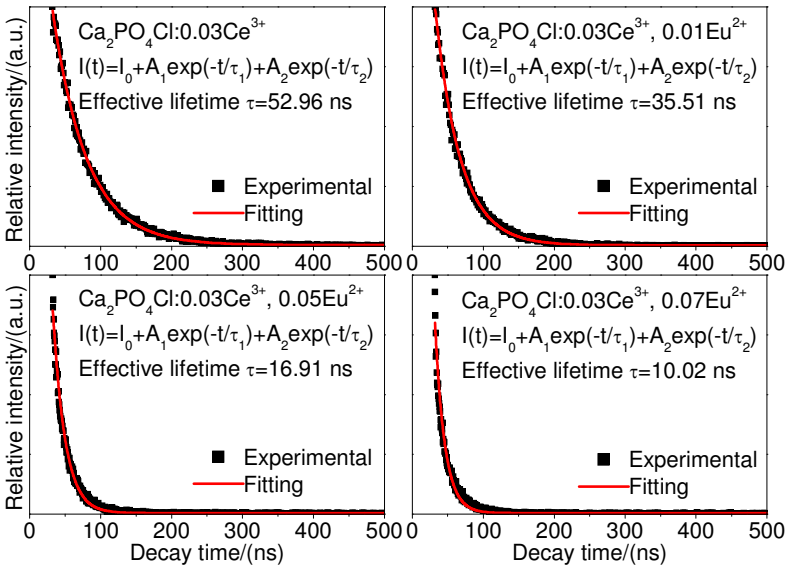

Fig.5. Decay curves of Ce^{3+} emission monitored at 367 nm for $Ca_2PO_4Cl:0.03Ce^{3+}$, yEu^{2+} (λ_{ex}=334 nm).

To further validate the process of energy transfer, the fluorescence lifetimes, τ, for Ce^{3+} with the

different Eu^{2+} doping content are measured, as a representative, the results of Ca_2PO_4Cl:0.03Ce^{3+}, Ca_2PO_4Cl:0.03Ce^{3+}, 0.01Eu^{2+}, Ca_2PO_4Cl:0.03Ce^{3+}, 0.05Eu^{2+} and Ca_2PO_4Cl:Ce^{3+}, 0.1Eu^{2+} are shown in Fig.5 (λ_{ex}=334 nm, λ_{em}=367 nm). The decay curves are well fitted with a second-order exponential decay mode by Eq.2 [34-36]

$$I=A_1\exp(-t/\tau_1)+A_2\exp(-t/\tau_2) \quad (2)$$

where I is the luminescence intensity; A_1 and A_2 are constants; t is the time, and τ_1 and τ_2 are the lifetimes for the rapid and slow decays, respectively. The average lifetimes (τ^*) can be calculated by the formula as follow [34-36]

$$\tau^*=(A_1\tau_1^2+A_2\tau_2^2)/(A_1\tau_1+A_2\tau_2) \quad (3)$$

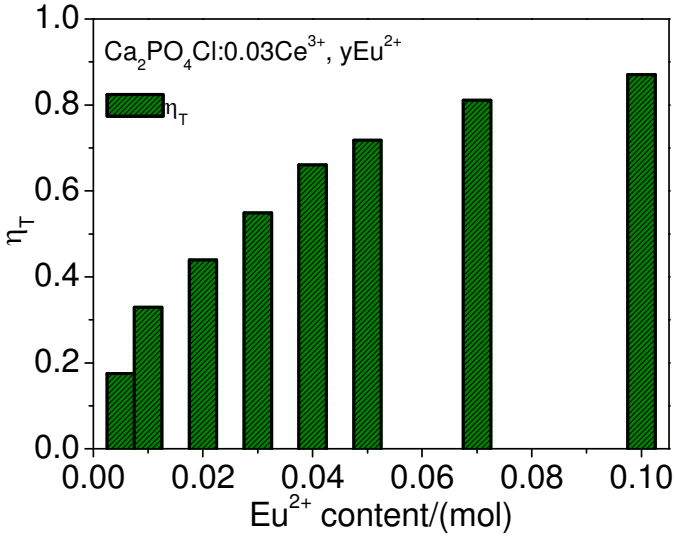

Fig.6. Variation of η_T for Ca_2PO_4Cl:0.03Ce^{3+}, $y$$Eu^{2+}$ (y=0-0.1) with the Eu^{2+} doping content.

For Ca_2PO_4Cl:0.03Ce^{3+}, $y$$Eu^{2+}$ (y=0-0.1), the calculated average lifetimes (τ^*) are 52.96, 43.69, 35.51, 29.68, 23.89, 17.98, 14.91, 10.02 and 6.87 ns, respectively. The energy transfer efficiency (η_T) can be calculated using the following equation by Paulose et al. [37-39]

$$\eta_T=1-(I_S/I_{S0})\approx1-(\tau_S/\tau_{S0}) \quad (4)$$

where τ_{S0} and τ_S are the decay lifetimes of the sensitizer Ce^{3+} in the absence and presence of the

activator Eu^{2+}. With increase the Eu^{2+} doping content, the η_T value is calculated and shown in Fig.6. And the energy transfer efficiency from Ce^{3+} to Eu^{2+} gradually increases with enhancing the Eu^{2+} doping content. At 0.1 mol Eu^{2+}, the energy transfer efficiency is 87.03%.

On the basis of Dexter's energy transfer formula for exchange and multipolar interactions, the following relation can be obtained [40-44]

$$\ln(\eta_0/\eta) \propto C \quad (5)$$

$$(\eta_0/\eta) \propto C^{\alpha/3} \quad (6)$$

where η_0 and η are the luminescence quantum efficiency of Ce^{3+} in the absence and presence of Eu^{2+}, respectively; C is the total doping content of the Ce^{3+} and Eu^{2+}. Eq.5 corresponds to the exchange interaction, and Eq.6 with α=6, 8, 10 corresponds to the dipole-dipole, dipole-quadrupole, and quadrupole-quadrupole interactions, respectively. Actually, for many codoped phosphors, the energy transfer mechanisms for exchange and multipolar interactions have already been discussed using Eq.5 and 6. For example, Guo et al. investigated the energy transfer mechanism of Eu^{2+}/Mn^{2+} codoped $Ca_9Lu(PO_4)_7$ [41], Shang et al reported the luminescence and energy transfer of Ce^{3+}/Eu^{2+} in $Ca_8La_2(PO_4)_6O_2$ [32]. Therefore, in the present work, the energy transfer mechanism of Ce^{3+}/Eu^{2+} in Ca_2PO_4Cl can also be explored by Eq.5 and 6. Because the value of η_0/η can be approximately estimated from the correlated lifetime ratio (τ_{S0}/τ_S), hence Eq.5 and 6 can be changed as follows

$$\ln(\tau_{S0}/\tau_S) \propto C \quad (7)$$

$$(\tau_{S0}/\tau_S) \propto C^{\alpha/3} \quad (8)$$

The relationships of $\ln(\tau_{S0}/\tau_S) \propto C$ and $(\tau_{S0}/\tau_S) \propto C^{\alpha/3}$ are illustrated in Fig.7. By consulting the fitting factor R, the relation $(\tau_{S0}/\tau_S) \propto C^{6/3}$ has the best fitting, implying that the dipole-dipole interaction is applied for the energy transfer from Ce^{3+} to Eu^{2+}.

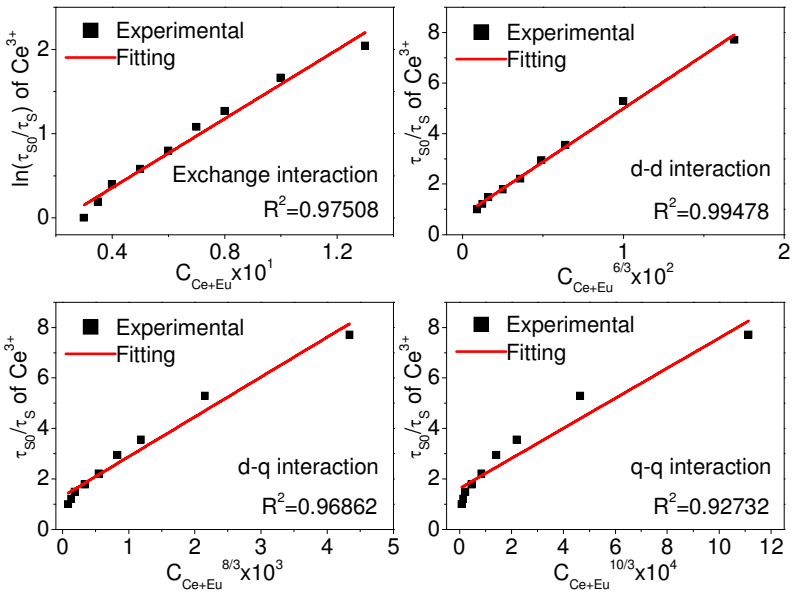

Fig.7. Dependence of $\ln(\tau_{S0}/\tau_S)$ of Ce^{3+} on (a) C and τ_{S0}/τ_S of Ce^{3+} (b) $C^{6/3}$, (c) $C^{8/3}$, and (d) $C^{10/3}$.

In general, the critical distance (R_c) can be calculated by the concentration quenching method. The critical distance $R_{Ce\text{-}Eu}$ between Ce^{3+} and Eu^{2+} can be estimated by [45]

$$R_{Ce\text{-}Eu}=2[3V/(4\pi x_c N)]^{1/3} \quad (9)$$

where x is the sum concentration of Ce^{3+} and Eu^{2+}, N is the number of Z ions in the unit cell (for Ca_2PO_4Cl, N=4), and V is the volume of the unit cell (for Ca_2PO_4Cl, V=0.46731 nm^3).

The estimated distance ($R_{Ce\text{-}Eu}$) for Ca_2PO_4Cl:0.03Ce^{3+}, $y$$Eu^{2+}$ phosphors (x_c=0.03, 0.035, 0.04, 0.05, 0.06, 0.07, 0.08, 0.1 and 0.13) are 1.95, 1.85, 1.77, 1.65, 1.55, 1.47, 1.41, 1.31 and 1.20 nm, respectively. The distances between Ce^{3+} and Eu^{2+} become shorter with increasing the Eu^{2+} doping content. x is the critical concentration at which the emission intensity of the donor (Ce^{3+}) in the presence of the acceptor (Eu^{2+}) is half that in the absence of the acceptor (Eu^{2+}). Therefore, the critical distance (R_c) of energy transfer is calculated to be about 1.77 nm for Ca_2PO_4Cl:0.03Ce^{3+}, y Eu^{2+}. $R_{Ce\text{-}Eu}$ for various Eu^{2+} content levels is much larger than the typical critical distance for the exchange interaction (0.5 nm) [46]. The results indicate that the exchange interaction plays no role in

the energy transfer process for $Ca_2PO_4Cl:0.03Ce^{3+}$, yEu^{2+}. Therefore, the energy transfer between Ce^{3+} and Eu^{2+} exists in Ca_2PO_4Cl, and the emission intensities of Eu^{2+} are obviously enhanced by the efficient energy transfer from Ce^{3+} to Eu^{2+}, which belongs to the multipolar interaction.

3.3 Thermal stability and CIE coordinates $Ca_2PO_4Cl:Ce^{3+}$, Eu^{2+}

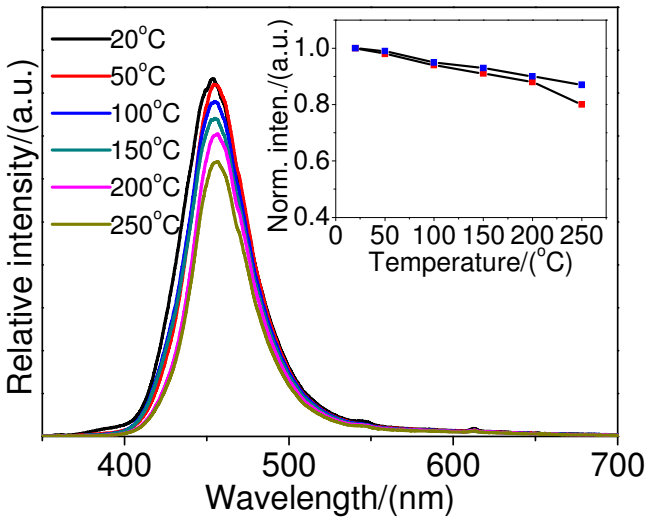

Fig.8. Temperature-dependent emission spectra of $Ca_2PO_4Cl:0.03Ce^{3+}$, $0.07Eu^{2+}$ (λ_{ex}=370 nm).

Inset: Normalized intensity of $Ca_2PO_4Cl:0.03Ce^{3+}$, $0.07Eu^{2+}$ and BAM as function of temperature (λ_{ex}=370 nm).

For the application of high power LEDs, the thermal stability of phosphor is one of important issues to be considered. For $Ca_2PO_4Cl:0.03Ce^{3+}$, $0.07Eu^{2+}$, the temperature dependence of emission spectra under the 370 nm radiation excitation is shown in Fig.8. The activation energy (E_a) can be expressed by [20, 47]

$$\ln(I_0/I)=\ln A-E_a/kT \quad (10)$$

where I_0 and I are the luminescence intensity of $Ca_2PO_4Cl:Ce^{3+}$, Eu^{2+} at room temperature and the testing temperature, respectively. A is a constant; k is the Boltzmann constant (8.617×10^{-5} eV K^{-1}). E_a is achieved to be 0.0114 eV K^{-1}. The inset depicts and compares the thermal quenching properties of $Ca_2PO_4Cl:Ce^{3+}$, Eu^{2+} and BAM. We observed only 6% decay at 100 ℃ for $Ca_2PO_4Cl:Ce^{3+}$, Eu^{2+},

as shown in Fig.8, $Ca_2PO_4Cl:Ce^{3+}$, Eu^{2+} has thermal quenching as good as that of BAM.

Color coordinates are one of the important factors for evaluating phosphors' performance, and the chromatic standard issued by the Commission Internationale de I'Eclairage in 1931 (CIE 1931). For $Ca_2PO_4Cl:0.03Ce^{3+}$, $0.07Eu^{2+}$, the CIE color coordinates are (0.1454, 0.0448). It can be seen that the color coordinates of $Ca_2PO_4Cl:0.03Ce^{3+}$, $0.07Eu^{2+}$ are about the blue region. The all results also indicate that $Ca_2PO_4Cl:Ce^{3+}$, Eu^{2+} may be a potential blue phosphor for the high-LED application.

4 Conclusions

In summary, $Ca_2PO_4Cl:Ce^{3+}$, Eu^{2+} phosphors are synthesized by the conventional solid state method. $Ca_2PO_4Cl:Ce^{3+}$, Eu^{2+} can produce two emission bands, which correspond to the $4f^0 5d^1 \rightarrow 4f^1$ transition of Ce^{3+} ion and the $4f^6 5d^1 \rightarrow 4f^7$ transition of Eu^{2+} ion, respectively. The energy transfer $Ce^{3+} \rightarrow Eu^{2+}$ in Ca_2PO_4Cl has been validated and proved to be a resonant type via the dipole-dipole interaction. The thermal quenching property reveals that $Ca_2PO_4Cl:Ce^{3+}$, Eu^{2+} has an excellent characteristics. Based on the results, we are currently evaluating the potential application of $Ca_2PO_4Cl:Ce^{3+}$, Eu^{2+} as a blue-emitting n-UV convertible phosphor.

Supporting Information

Fig.S1, emission spectra of $Ca_2PO_4Cl:0.03Ce^{3+}$ and $Ca_2PO_4Cl:0.03Ce^{3+}$, $0.03Na^+$. Fig.S2, emission spectra of $Ca_2PO_4Cl:0.07Eu^{2+}$, $Ca_2PO_4Cl:0.03Ce^{3+}$, $0.07Eu^{2+}$ and $BaMgAl_{10}O_{17}:Eu^{2+}$.

Acknowledgments

The work is supported by the National Natural Science Foundation of China (No. 50902042), the Natural Science Foundation of Hebei Province, China (No.A2014201035; E2014201037) and the Education Office Research Foundation of Hebei Province, China (Nos.ZD2014036; QN2014085).

References

[1] Guo N.; Jia Y.; Lü W.; Lv W.; Zhao Q.; Jiao M.; Shao B.; You H. Dalton Trans. 2013, 42, 5649-5654.

[2] Yeh C.-W.; Chen W.-T.; Liu R.-S.; Hu S.-F.; Sheu H.-S.; Chen J.-M.; Hintzen H. T. J. Am. Chem. Soc. 2012, 134, 14108-14117.

[3] Hou D.; Liu C.; Ding X.; Kuang X.; Liang H.; Sun S.; Huang Y.; Tao Y. J. Mater. Chem. C 2013, 1, 493-499.

[4] Pradal N.; Chadeyron G.; Thérias S.; Potdevin A.; Santilli C. V.; Mahiou R. Dalton Trans. 2014, 43, 1072-1081.

[5] Ray S.; Fang Y.-C.; Chen T.-M. RSC Adv. 2013, 3, 16387-16391.

[6] Tao Z.; Huang Y.; Seo H. J. Dalton Trans. 2013, 42, 2121-2129.

[7] Zhou J.; Xia Z.; Yang M.; Shen K. J. Mater. Chem. 2012, 22, 21935-21941.

[8] Song H. J.; Yim D. K.; Roh H.-S.; Cho I. S.; Kim S.-J.; Jin Y.-H.; Shim H.-W.; Kim D.-W.; Hong K. S. J. Mater. Chem. C 2013, 1, 500-505.

[9] Liu W.-R.; Huang C.-H.; Wu C.-P.; Chiu Y.-C.; Yeh Y.-T.; Chen T.-M. J. Mater. Chem. 2011, 21, 6869-6874.

[10] Wang Q.; Deng D.; Hua Y.; Huang L.; Wang H.; Zhao S.; Jia G.; Li C.; Xu S J. Lumin. 2012, 132, 434-438.

[11] Fang Y.; Li L.; Chen Y.; Wang H.; Zeng R. J. Lumin. 2013, 144, 13-17.

[12] Song X.; Fu R.; Agathopoulos S.; He H.; Zhao X.; Li R. J. Electrochem. Soc. 2010, 157, J34-J38.

[13] Fu R.; Agathopoulos S.; Song X.; Zhao X.; He H.; Yu X. Opt. Mater. 2010, 33, 99-102.

[14] Sun J.; Zeng J.; Sun Y.; Du H. J. Alloys Compd. 2012, 540, 81-84.

[15] Shang M.; Geng D.; Zhang Y.; Li G.; Yang D.; Kang X.; Lin J. J. Mater. Chem. 2012, 22, 19094-19104.

[16] Lan L.; Feng H.; Tang Y.; Tang W. Opt. Mater. 2011, 34, 175-178.

[17] Huang C.-H.; Luo L.; Chen T.-M. J. Electrochem. Soc. 2011, 158, J341-J344.

[18] Tang W.; Chen D.; Yang H. Appl. Phys. A 2013, 103, 263-266.

[19] Wang Z.; Teng X.; Li P. J. Alloys Compud. 2014, 589, 549-552.

[20] Chiu Y.-C.; Liu W.-W.; Chang C.-K.; Liao C.-C.; Yeh Y.-T.; Jang S.-M.; Chen T.-M. J. Mater. Chem. 2010, 20, 1755-1758.

[21] Meijering A.; Blasse G. J. Phys.: Condens. Matter 1990, 2, 3619-3628.

[22] Yu R.; Guo C.; Li T.; Xu Y. Curr. Appl. Phys. 2013, 13, 880-884.

[23] Wang Z.; Li P.; Yang Z.; Guo Q. J. Lumin. 2014, 151, 170-175.

[24] Greenblatt M.; Banks E.; Post B. Acta Crystallographica 1967, 23, 166-171.

[25] Greenblatt M.; Banks E.; Post B. Acta Crystallographica section B 1969, 25, 2170-2171.

[26] Jiao M.; Jia Y.; Lü W.; Lv W.; Zhao Q.; Shao B.; You H. Dalton Trans. 2014, 43, 3202-3209.

[27] Liu H.; Liao L.; Xia Z. RSC Adv. 2014, 4, 7288-7295.

[28] Dutta S.; Som S.; Sharma S. K. Dalton Trans. 2013, 42, 9654-9661.

[29] Paulose P. I.; Jose G.; Thomas V.; Unnikrishnan N. V.; Warrier M. K. R. J. Phys. Chem. Solids 2003, 64, 841-846.

[30] Lv W.; Jia Y.; Zhao Q.; Jiao M.; Shao B.; Lv W.; You H. RSC Adv. 2014, 14074-14080.

[31] Lv W.; Jia Y.; Zhao Q.; Jiao M.; Shao B.; Lü W.; You H. RSC Adv. 2014, 4, 7588-7593.

[32] Shang M.; Li G.; Geng D.; Yang D.; Kang X.; Zhang Y.; Lian H.; Lin J. J. Phys. Chem. C 2012, 116, 10222-10231.

[33] Xia Z.; Liu R.-S. J. Phys. Chem. C 2012, 116, 15604-15609.

[34] Lv W.; Lü W.; Guo N.; Jia Y.; Zhao Q.; Jiao M.; Shao B.; You H. Dalton Trans. 2013, 42, 13071-13077.

[35] Huang C.-H.; Chen T.-M.; Liu W.-R.; Chiu Y.-C.; Yeh Y.-T.; Jang S.-M. ACS Appl. Mater. Interfaces 2010, 2, 259-264.

[36] Huang C.-H.; Chen T.-M. J. Phys. Chem. C 2011, 115, 2349-2355.

[37] Yang W.-J.; Chen T.-M. Appl. Phys. Lett. 2006, 88, 101903.

[38] Kwon K. H.; Im W. B.; Jang H. S.; Yoo H. S.; Jeon D. Y. Inorg. Chem. 2009, 48, 11525-11532.

[39] Li G.; Zhang Y.; Geng D.; Shang M.; Peng C.; Cheng Z.; Lin J. ACS Appl. Mater. Interfaces 2012, 4, 296-305.

[40] Dexter D. L.; Schulman J. H. J. Chem. Phys. 1954, 22, 1063-1070.

[41] Guo N.; Huang Y.; You H.; Yang M.; Song Y.; Liu K.; Zheng Y. Inorg. Chem. 2010, 49, 10907-10913.

[42] Reisfeld R.; Greenberg E.; Velapoldi R.; Barnett B. J. Chem. Phys. 1972, 56, 1698-1705.

[43] Caldiño U.; Hernández-Pozos J. L.; Flores C.; Speghini A.; Bettinelli M. J. Phys.: Condens. Matter 2005, 17, 7297-7306.

[44] Martínez-Martínez R.; García M.; Speghini A.; Bettinelli M.; Falcony C.; Caldiño U. J. Phys.: Condens. Matter 2008, 20, 395205.

[45] Blass G. Philips Res. Rep. 1969, 24, 131-144.

[46] Blasse G.; Grabmaier B. C. Luminescent Materials, Berlin: Springer, 1994.

[47] Huang C.-H.; Chen Y.-C.; Chen T.-M.; Chan T.-S.; Sheu H.-S. J. Mater. Chem. 2011, 21, 5645-5649.